$$\mathbf{N} = \begin{bmatrix} [2M_7\beta_{2S}\dot{\delta} + 4M_6\delta\dot{\delta} + (M_u/2)\sum_i W_i\dot{W}_i](\dot{\beta} + \dot{\theta} + \omega_0) - I_5(\dot{\theta} + \omega_0)^2 \\ I_5(\dot{\beta} + \dot{\theta} + \omega_0)^2 + [(M_u/2)\sum_i W_i\dot{W}_i - 2I_6\dot{\delta}](\dot{\theta} + \omega_0) + 2I_6\dot{\delta}\dot{\beta} \\ [I_5 + M_7\beta_{2c} - M_T\delta + (M_u/4)W_1](\dot{\theta} + \omega_0)^2 \\ [I_6 + M_7\beta_{2c} - M_T\delta + (M_u/4)W_2](\dot{\theta} + \omega_0)^2 \\ \vdots \\ 0 \end{bmatrix} \quad \text{(A5)}$$

where the M and I parameters are tabulated in Table 2.

References

[1] Gatlin, J. A. et al., "Satellite Attitude Control Using A Torqued, Two-axis-gimballed Boom as the Actuator," AIAA Paper 68-857, Pasadena, Calif., 1968.

[2] Graham, J. D., "Dynamics of a Satellite Having Long Flexible Extendible Members," *Proceedings of the XVII International Astronautical Congress*, Madrid, Spain, Oct. 1966, pp. 163–178.

[3] Dow, P. C. et al., "Dynamic Stability of a Gravity-Gradient Stabilized Satellite Having Long Flexible Antennas," *Proceedings of the AIAA Guidance and Control Specialists Conference*, Seattle, Wash., Aug. 1966, pp. 285–303.

[4] Hooker, W. W. and Marqulies, G., "The Dynamical Attitude Equations For An N-body Satellite," *Journal of the Astronautical Sciences*, Vol. 12, No. 4, Winter 1965, pp. 122–128.

[5] Roberson, R. E., and Wittenburg, J., "A Dynamical Formalism for an Arbitrary Number of Interconnected Bodies, With Reference to the Problem of Satellite Attitude Control," paper 46.D, June 1966, International Federation on Automatic Control, London, England.

[6] Ashley, H., "Observations on the Dynamic Behavior of Large Flexible Bodies in Orbit," *AIAA Journal*, Vol. 5, No. 3, March 1967, pp. 460–469.

[7] Liu, H. S. and Mitchell, T. P., "Resonant Oscillations of a Flexible Satellite in an Elliptic Orbit," *AIAA Journal*, Vol. 5, No. 7, July 1967, pp. 1269–1272.

[8] Newton, J. K. and Farrell, J. L., "Natural Frequencies of a Flexible Gravity-Gradient Satellite," *Journal of Spacecraft and Rockets*, Vol. 5, No. 5, May 1968, pp. 566–569.

[9] Hurty, W. C. and Rubinstein, M. F., *Dynamics of Structures*, 1st ed., Prentice-Hall, Englewood Cliffs, N. J., 1965, pp. 4–7.

[10] Greenwood, D. T., *Principles of Dynamics*, Prentice-Hall, Englewood Cliffs, N. J., 1965, p. 256.

[11] Felgar, R. P., "Formulas for Integrals Containing Characteristic Functions of a Vibrating Beam," Research Circular 14, 1950, Univ. of Texas Bureau of Engineering.

[12] Likins, P. W., "Use of Synthetic Modes in Hybrid Coordinate Dynamic Analysis," *AIAA Journal*, Vol. 6, No. 10, Oct. 1968, pp. 1867–1872.

MARCH 1970 J. SPACECRAFT VOL. 7, NO. 3

A Simple Description of Combined Precession and Nutation in an N-Member System of Coaxial, Differentially Spinning Bodies

DONALD J. LISKA*

University of California, Los Alamos Scientific Laboratory, Los Alamos, N. Mex.

The spin axis motion of an n-body, coaxially-mounted cluster of differentially spinning bodies is analyzed. The description of this motion is made as simple as possible by linearizing the coordinate transformation equations. The resulting motions are then restricted to 10° or so (an acceptable assumption for many applications). The epicycloidal motion is discussed by means of computer plots for different values of momentum, inertia, and torque. Equivalent single bodies with dynamic responses similar to the coaxial system are described. A simple graphical method can be used to plot the spin axis motion for all cases.

Nomenclature

x,y,z = coordinates of body to which torque is applied
ω_x,ω_y = x and y axis angular rates of body of x,y,z coordinates
φ = spin rate of body with x,y,z coordinates
A = transverse inertia of body with x,y,z coordinates
C = axial inertia of body with x,y,z coordinates
H = angular momentum of body with x,y,z coordinates
A_c = transverse inertia of rest of system
H_c = spin axis angular momentum of rest of system
H_0 = total spin axis angular momentum
T_x = torque applied about x axis of body with x,y,z coordinates
T_{xR},T_{yR} = reaction torques about x and y axes
$\Delta\theta,\Delta\mu$ = spin axis angles of deviation relative to inertial space
t_p = time duration of torque application, measured from zero
t = time variable for all cases
φ_e = spin rate of equivalent body
R_F = radius of fixed circle in graphical method
R_R = radius of rolling circle in graphical method

Received January 13, 1969; revision received November 10, 1969. The majority of this work was accomplished while the author was employed at The Boeing Company, under sponsorship of the Aerospace Division, Research and Development. This work was also supported in part by the U.S. Atomic Energy Commission.

*Professor.

Introduction

THE usefulness of a first-order linear analysis in understanding the basic characteristics of motion of spinning bodies in space has beeen well demonstrated. In particular, such an analysis can be used to describe the spin-axis motion of a cluster of symmetrical bodies, coaxially mounted, and spin-

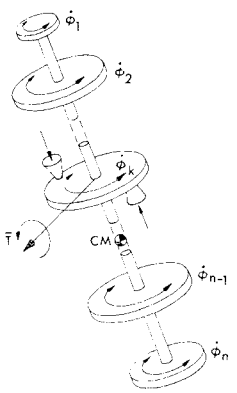

Fig. 1 A system of coaxial differentially spinning bodies with torque T applied to body k.

ning at different speeds in either direction, when the system is acted upon by a torque vector spinning with any one body of the system. This sort of dynamics problem has become of interest with the introduction of dual space system concepts involving coaxial, differentially spinning stages for such purposes as housing an instrument package on a despun or slowly spinning stage while benefiting from the stability provided by another stage with a higher angular momentum content.[1-4]

This paper describes the relationship of the spin axis of an n-body coaxial system to a fixed point in space as a torque is applied to any one body of the system. It is shown that the spin axis traces an epicycloid in space. The number of cusps in this epicycloid is shown to be a function of the spin rate of the body being torqued and the nutation rate of the over-all system. Expressions are derived for the maximum nutation amplitude following a given torque period, the net attitude change resulting in the spin axis following nutation damping, and the torque angles which result in maximum and zero nutation. The epicycloid is shown to reduce to a cardioid for a single body with an axial to transverse inertia ratio equal to 2.0. An equivalent single body is described which produces the same motion as the coaxial-differentially spinning system if a torque is applied at a rate other than the spin rate. Alternatively, a fictitious single body not restricted in inertia ratio by the limits 0 and 2.0 can also duplicate this motion. Numerous computer plots are shown to clarify the subtleties of the motions with different combinations of system parameters. A simple graphical method is described which can also be used to plot the spin axis motion for all cases.

Problem Description

A linear analysis will be made of the system shown in Fig. 1. The assumption is made that all n bodies are symmetrical about the spin axis; that is, their individual mass distributions are such that the transverse inertia of each body is the same for all axes which intersect the spin axis in a plane perpendicular to the spin axis. This also necessitates that the mass center of each body lie on the spin axis. The torque is applied to only one body of the system, and it is fixed relative to that body. The coordinates of this body are x,y,z. The torque is a step constant, applied at time zero for a duration t_p.

The conversion of angular rates in body coordinates to angular motions in inertial coordinates is made by means of the coordinate transformation in Fig. 2. The interpretation of these inertial angular motions is made with the rectangular grid shown in Fig. 3 where $\Delta\theta$ and $\Delta\mu$ are restricted to small "angles," i.e., less than $\pm 10°$, for which the analysis is sufficiently accurate. The initial condition is stable spin about the inertially fixed reference axis, i.e., zero initial angular rates in either the $\Delta\theta$ or $\Delta\mu$ directions.

Since the torque vector is attached to any body of the system, it does not matter if the x,y,z coordinates of this body pass through the center of mass of the system. In general they will not. The rotational motion occurs about the system center of mass in either case for a free body and the angles computed are the same. If the torque is not a pure couple, small translational motions will occur which again do not influence the rotation.

Equations of Motion

The equations of motion are derived from Euler's equations. These are written for the body which carries the torque vector and which rotates at an angular rate $\dot{\varphi}$,

$$T_x + T_{xR} = A\dot{\omega}_x + (C - A)\dot{\varphi}\omega_y \quad (1)$$

$$T_{yR} = A\dot{\omega}_y - (C - A)\dot{\varphi}\omega_x \quad (2)$$

Where a symmetrical mass distribution about the rotation axis has been assumed for all bodies in the system. T_x is the torque applied directly by the motors and T_{xR} and T_{yR} are x and y axis reaction torques between body j and all the other bodies of the system. These other bodies can be looked upon as a composite gyro rotor which precesses in space due only to the reaction torques applied by the torquer body,

$$-\bar{T}_R = \dot{\bar{H}} = d/dt(A_c\omega_x\bar{a}_x + A_c\omega_y\bar{a}_y + H_c\bar{a}_z) = A_c\dot{\omega}_x\bar{a}_x + A_c\dot{\omega}_y\bar{a}_y + A_c\omega_x(\bar{\omega} \times \bar{a}_x) + A_c\omega_y(\bar{\omega} \times \bar{a}_y) + H_c(\bar{\omega} \times \bar{a}_z) \quad (3)$$

Expanding Eq. (3) gives T_{xR} and T_{yR},

$$T_{xR} = -A_c\dot{\omega}_x + A_c\omega_y\dot{\varphi} - H_c\omega_y \quad (4)$$

$$T_{yR} = -A_c\dot{\omega}_y - A_c\omega_x\dot{\varphi} + H_c\omega_x \quad (5)$$

Substituting into Eqs. (1) and (2) gives the equations of motion in body coordinates

$$T_x = A_s\dot{\omega}_x + (H_0 - A_s\dot{\varphi})\omega_y \quad (6)$$

$$O = A_s\dot{\omega}_y - (H_0 - A_s\dot{\varphi})\omega_x \quad (7)$$

where $A_s = A + A_c = A + A_1 + A_2 + \ldots + A_n + Ml^2 + M_1l_1^2 + \ldots + M_nl_n^2$ = total transverse moment of inertia of the system measured about the center of mass.

$$H_0 = C\dot{\varphi} + H_c = C\dot{\varphi} + \sum_{j=1}^{n} C_j\dot{\varphi}_j$$

equals total angular momentum of the system measured about the spin axis.

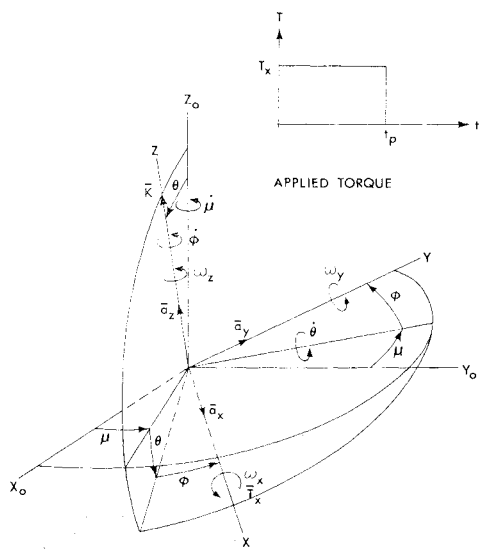

Fig. 2 Coordinate transformation diagram with torque T_x applied about the x-body axis.

Period of Torque Application ($0 < t < t_p$)

At the instant the torque is applied the coaxial system is assumed to be spinning without nutation. The solutions of Eqs. (6) and (7) for this initial state of stable spin, i.e., $\omega_x(0) = \dot{\omega}_x(0) = \omega_y(0) = \dot{\omega}_y(0) = 0$, are

$$\omega_x = (T_x/A_s\xi)\sin\xi t \tag{8}$$

$$\omega_y = (T_x A_s\xi)(1 - \cos\xi t) \tag{9}$$

where $\xi = (H_0/A_s) - \dot{\varphi}$.

The next step is to express these angular rates in terms of inertial coordinates by means of the following coordinate transformation equations derived from Fig. 2.

$$\omega_x = \dot{\theta}\mathrm{s}\varphi - \dot{\mu}\mathrm{s}\theta\mathrm{c}\varphi, \quad \omega_y = \dot{\theta}\mathrm{c}\varphi + \dot{\mu}\mathrm{s}\theta\mathrm{s}\varphi \tag{10}$$

where $\mathrm{s} \equiv \sin$, $\mathrm{c} \equiv \cos$. At this point, the problem is linearized by restricting increments of the transformation angles θ and μ to be small. By this means simple solutions reasonably accurate up to about 10° are obtained. The angle θ is allowed a small deviation $\Delta\theta$ about 90° rather than 0 ° in order that $\sin\theta \approx 1$. The angle μ deviates $\Delta\mu$ about °0. Thus, Eqs. (10) become

$$\omega_x = \dot{\theta}\mathrm{s}\varphi - \dot{\mu}\mathrm{c}\varphi, \quad \omega_y = \dot{\theta}\mathrm{c}\varphi + \dot{\mu}\mathrm{s}\varphi \tag{11}$$

Upon substituting into Eqs. (8) and (9) and integrating, expressions for the incremental changes in θ and μ, valid during the period of torque application, are obtained

$$\Delta\theta = -(T_x/A_s\xi)[(A_s/H_0)\mathrm{s}(H_0/A_s)t - (1/\dot{\varphi})\mathrm{s}\dot{\varphi}t] \tag{12}$$

$$\Delta\mu = (T_x/\dot{\varphi}H_0) + (T_x/A_s\xi)[(A_s/H_0)\mathrm{c}(H_0/A_s)t - (1/\dot{\varphi})\mathrm{c}\dot{\varphi}t] \tag{13}$$

Period Following Torque Application ($t > t_p$)

The post torque period is defined by $t - t_p > 0$. At the time of torque termination t_p, the values of ω_{xp} and ω_{yp} are found from Eqs. (8) and (9). The transformation equation, Eq. (11), accounting for the rotation of the x-y coordinates through angle $\dot{\varphi}t_p$ during the torque period becomes

$$[\omega_{xp}\mathrm{c}(\dot{\varphi}t_p) - \omega_{yp}\mathrm{s}(\dot{\varphi}t_p)]\mathrm{c}(\dot{\varphi}t) - [\omega_{xp}\mathrm{s}(\dot{\varphi}t_p) + \omega_{yp}\mathrm{c}(\dot{\varphi}t_p)]\mathrm{s}(\dot{\varphi}t) = \dot{\theta}\mathrm{s}(\dot{\varphi}t) - \dot{\mu}\mathrm{c}(\dot{\varphi}t) \tag{14}$$

$$[\omega_{xp}\mathrm{s}(\dot{\varphi}t_p) + \omega_{yp}\mathrm{c}(\dot{\varphi}t_p)]\mathrm{c}(\dot{\varphi}t) + [\omega_{xp}\mathrm{c}(\dot{\varphi}t_p) - \omega_{yp}\mathrm{s}(\dot{\varphi}t_p)]\mathrm{s}(\dot{\varphi}t) = \dot{\theta}\mathrm{c}(\dot{\varphi}t) + \dot{\mu}\mathrm{s}(\dot{\varphi}t) \tag{15}$$

By integrating these equations, the following expressions are obtained for $\Delta\theta$ and $\Delta\mu$, valid during all time following shutting off the torque:

$$\Delta\theta = \frac{T_x}{\dot{\varphi}H_0}\mathrm{s}\dot{\varphi}t_p + \frac{T_x}{H_0\xi}\left[\mathrm{s}\left(-\xi t_p + \frac{H_0}{A_s}t\right) - \mathrm{s}\frac{H_0}{A_s}t\right] \tag{16}$$

$$\Delta\mu = \frac{T_x}{\dot{\varphi}H_0}(1 - \mathrm{c}\dot{\varphi}t_p) - \frac{T_x}{H_0\xi}\left[\mathrm{c}\left(-\xi t_p + \frac{H_0}{A_s}t\right) - \mathrm{c}\frac{H_0}{A_s}t\right] \tag{17}$$

While Eqs. (16) and (17) are again reasonably accurate only up to 10° or so, the post-torque period angular rates in body coordinates may be found rigorously. This is done by using the initial conditions at $t = t_p$ and again solving Euler's equations:

$$\omega_x = -\frac{T_x}{A_s\xi}\left\{\mathrm{s}\left[\left(2\dot{\varphi} - \frac{H_0}{A_s}\right)t_p + \xi t\right] - \mathrm{s}(\dot{\varphi}t_p + \xi t)\right\} \tag{18}$$

$$\omega_y = -\frac{T_x}{A_s\xi}\left\{\mathrm{c}(\dot{\varphi}t_p + \xi t) - \mathrm{c}\left[\left(2\dot{\varphi} - \frac{H_0}{A_s}\right)t_p + \xi t\right]\right\} \tag{19}$$

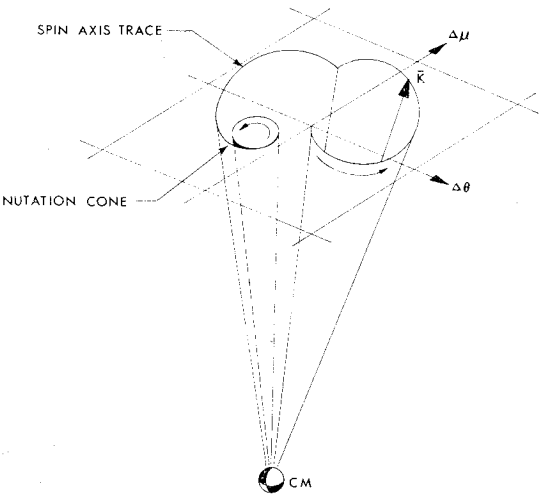

Fig. 3 Relation of the geometric spin axis to the inertial coordinate frame $\Delta\theta$-$\Delta\mu$ for small angles.

Trace of Spin Axis

In the foregoing equations, two distinct angular frequencies are evident; $\dot{\varphi}$, the spin rate of the body which is applying torque to the system and H_0/A_s, the nutation frequency of the overall system. Nutation is a measure of the excess angular kinetic energy in a system, or mathematically, a misalignment of the angular momentum and angular velocity vectors. If no external torque is applied to the system, the angular momentum vector remains fixed and of constant magnitude in inertial space. If the system nutates, excess rotational kinetic energy is present which can be dissipated passively, i.e., by conversion of the excess energy to heat through friction, and the body will then spin without nutation about an axis aligned with the momentum vector. Thus, nutation damping is inherent in any dissipative system as the system tends toward a minimum energy state in measure with its momentum.

The motion of the tip of the spin axis in inertial space is a combination of spin and nutation and has all the properties of an epicycloid as long as the torque is applied. This is shown in Fig. 3. When the torque is cut off, circular nutation motion takes place and the spin axis traces out a conical path about the now stationary momentum vector. Specific characteristics of these motions can easily be derived.

1) Circular motion of the momentum vector. The tip of the momentum vector moves in a circular path when T_x is held on and constant. This path always intersects the origin for the initial conditions used in the above derivations. This path is defined by the steady-state parts of Eqs. (16) and (17):

$$\Delta\theta = (T_x/\dot{\varphi}H_0)\mathrm{s}\dot{\varphi}t_p \quad \Delta\mu = (T_x/\dot{\varphi}H_0)(1 - \mathrm{c}\dot{\varphi}t_p) \tag{20}$$

This defines a point moving about a circle of diameter $2T_x/\dot{\varphi}H_0$ with a frequency $\dot{\varphi}$ and passing through the origin each cycle. The momentum vector thus moves at the same speed that the torque vector rotates and stops moving at the instant the torque is shut off. If the instantaneous angular velocity vector is not aligned with the momentum vector at this instant, the body will then nutate about the position defined by Eqs. (20) at t_p. If dissipation is present, this nutation will exponentially decay until stable spin around the momentum vector is achieved.

2) Nutation cusps Nutation amplitude at any time is found by subtracting the momentum vector position given by Eqs. (20) from the instantaneous spin axis position during the torque period as given by Eqs. (12) and (13). The amplitude is found from the rss of this difference for each axis

$$\text{deviation at time } t_p = -(T_x/H_0\xi)(2 - 2\mathrm{c}\xi t_p)^{1/2} \tag{21}$$

$$\text{maximum deviation} = |2T_x/H_0\xi|\text{rad} \tag{22}$$

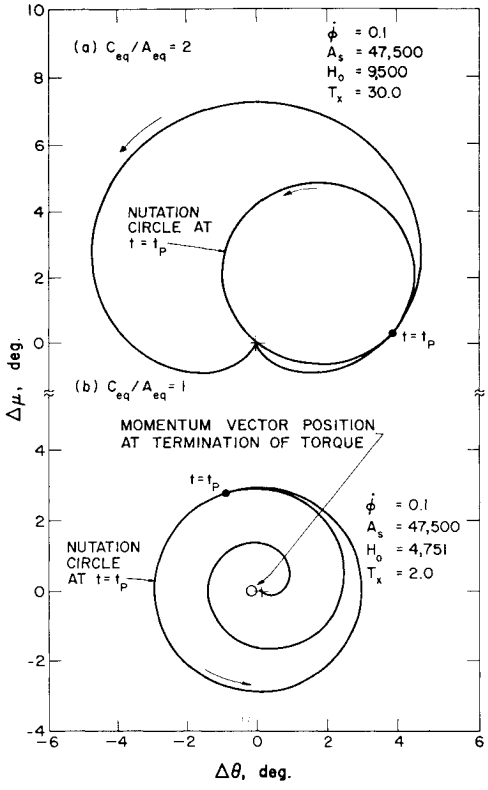

Fig. 4 a) Cardioid motion for "thin disk" configuration; b) motion of nonnutating "spherical" configuration.

This frequency of this deviation is the difference between the nutation rate and the spin rate. The number of cusps of nutation can thus be found by dividing this difference by the spin rate.

$$\text{cusps per cycle} = |\xi/\dot\varphi| = |1 - (H_0/\dot\varphi A_s)| \qquad (23)$$

where the absolute value is taken to avoid confusion when $H_0/\dot\varphi A_s > 1$, although this certainly influences the number of cusps.

3) Angles of zero and maximum nutation For attitude control purposes, it is useful to know the torque angles $\dot\varphi t_p$ which result in zero nutation, i.e., the points at which the angular velocity and angular momentum vectors are instantaneously aligned. From Eq. (23), zero deviation occurs when

$$1 - c\xi t_p = 0, \text{ or } \dot\varphi t_p = |n\pi/[(H_0/A_s\dot\varphi) - 1]|, n = 0,2,4, \ldots \qquad (24)$$

Similarly, maximum deviation occurs when

$$\dot\varphi t_p = |n\pi/[(H_0/A_s\dot\varphi) - 1]|, n = 1,3,5, \ldots \qquad (25)$$

With Eqs. (20–25), all of the important characteristics of the spin axis motion for any set of coaxial system parameters can be computed.

Coaxial System Interpreted as an Equivalent Single Body

Before proceeding with sample solutions of the equations, it is useful to consider what is involved in interpreting the coaxial system as an equivalent single spinning body. If the rotational rates are the same for each member of the coaxial system, then the response to the applied torque will be exactly the same as for a single rigid body. In this case, $H_0 = (C + C_1 + C_2 + \ldots + C_n)\dot\varphi$ and the nutation frequency is $(C + C_1 + C_2 + \ldots + C_n)\dot\varphi/A_s$. Obviously, the inertia ratio $(C + C_1 + C_2 + \ldots + C_n)/A_s$ lies, in this case, between the limits of 0 and +2, for if the bodies were mounted on an extremely long shaft, the radius of gyration would make $A_s \gg C$ total and the ratio would approach zero in the limit. If, on the other hand, the system is very compact with a relatively small radius of gyration and the bodies are all thin discs, then $A_s \approx 0.5\,C$ total for which the inertia ratio never exceeds +2. In the first case, the system possesses no gyroscopic stability and it responds as a static body of transverse inertia A_s to a torque vector rotating at angular rate $\dot\varphi$. In the second case, the system will respond as a cardioid, where zero nutation occurs at $\dot\varphi t = 0, 2\pi, \ldots$ and maximum nutation at $\dot\varphi t = \pi, 3\pi, \ldots$. For the cardioid, the nutation circles will always pass through the origin regardless of t_p.

A more general interpretation is possible which places no restrictions on the spin of the various members of the coaxial system. In this case, the torque vector still rotates at speed $\dot\varphi$, but it acts upon an equivalent body which rotates at a different speed $\dot\varphi_e$. If this equivalent body is assumed to have a spin inertia equal to the arithmetic sum of the spin inertias of the coaxial members and its spin momentum is required to be equal to H_0, the spin rate must be

$$\dot\varphi_e = \left[\left(1 + \sum_{j=1}^{n} \frac{C_j\dot\varphi_j}{C\dot\varphi}\right)\Big/\left(1 + \sum_{j=1}^{n} \frac{C_j}{C}\right)\right]\dot\varphi \qquad (26)$$

The speed of the equivalent single body, therefore, lies between the speeds of the coaxial members, and its value is determined by the weighted mean of angular momentum. If now this body is acted upon by a torque which rotates vector wise at the speed $\dot\varphi$, the spin axis motion of any coaxial system can be duplicated.

Still a third interpretation requires that the equivalent single body have the same nutation frequency and angular momentum as the coaxial system. If the equivalent body is assumed to spin at the reference rate $\dot\varphi$, then the equivalent inertia ratio must be

$$C_e/A_e = \left|\left(C + \sum_{j=1}^{n} \frac{C_j\dot\varphi_j}{\dot\varphi}\right)\Big/A_s\right| \qquad (27)$$

It can be seen that if no restrictions are placed on the spin speeds in Eq. (27), the equivalent inertia ratio must be allowed to range from $-\infty$ to $+\infty$. This is a peculiar situation, because it implies that this equivalent body can have a nutation frequency greater than twice the spin rate. Of course, this is not physically possible, so for any "real" body a speed restriction must be placed on $\dot\varphi$ as follows:

$$-\sum_{j=1}^{n} \frac{C_j\dot\varphi_j}{C} \le \dot\varphi \le \frac{2A_e}{C}\,\dot\varphi - \sum_{j=1}^{n} \frac{C_j\dot\varphi_j}{C} \qquad (28)$$

Equation (28) is merely a formalization of the rule, $0 \le C_e/A_e \le 2$. The lower limit in Eq. (28) represents the point at which total system momentum is zero which may result from counter rotation in the system. Further counter rotation would make momentum negative relative to $\dot\varphi$, but this situation cannot be duplicated by the equivalent body. The upper limit is where the nutation frequency equals $2\dot\varphi$ and a further increase in momentum again produces motions which cannot be duplicated by the equivalent body.

Although the interpretation of a "real" equivalent single body must be restricted in this manner, the concept of a theoretical body with $-\infty < C_e/A_e < +\infty$ will be useful in explaining the examples to follow and describing a graphical method of tracing spin axis motion for any set of coaxial system parameters.

Sample Solutions of the Equations of Motion

Let us first consider a system with a total transverse inertia about the center of mass, A_s = 47,500 ft-lb-sec^2. Let the spin rate of the body to which the torque vector is affixed be $\dot\varphi$ = 0.1 rad/sec. Assume these two parameters to be fixed,

and vary H_0, T_x, and t_p, in order to study the different motions involved.

case 1: $0 \leq H_0 \leq +9500$ ft-lb-sec $(0 \leq C_e/A_e \leq 2)$

For this range of spin axis momentum (net H_0 in same direction as $\dot{\varphi}$), the coaxial system will respond as a "real" single body which varies in shape between a thin rod and a thin disk. In Fig. 4a is shown a cardioid corresponding to the upper H_0 limit. Interestingly enough, exactly the same pattern is also obtained for $H_0 = +2375$ $(C_e/A_e = 0.5)$, but in the latter case the spin axis sweeps out its pattern at half the speed because the nutation frequency H_0/A_s is half as great. In both cases, the nutation circles pass through the origin as stated earlier, regardless of when the torque is terminated. When $H_0 = 4750$ $(C_e = A_e)$, gyroscopic stability is lost and the system responds to the torque as a sphere would with every increasing divergence of the "geometric" spin axis in a spiral path (within small angle limitations). In this case, the system does not nutate when the torque is shut off. The geometric axis proceeds to move about the terminal position of the momentum vector in a perfect circle which implies that the body is spinning without nutation about the momentum vector, i.e., $\bar{\omega}$, the total angular velocity vector, is aligned with $\bar{H}$, the total system momentum vector. This situation is shown in Figs. 4b and 5.

If H_0 is reduced to nearly zero, the radius of the circular path of the momentum vector becomes very large by Eq. (20). Whatever value it assumes for a small but nonzero H_0, the maximum deviation of the spin axis from the momentum circle approaches twice this value, and the number of nutation cusps approaches 1. Thus, the body will diverge on a closed path of immense size.

case 2: $H_0 > +9500$ ft-lb-sec $(2 < C_e/A_e < +\infty)$

This range of H_0 produces motions not possible with a single body having an "attached" torque vector. The motion is more complex in this case, but it can easily be predicted by means of Eqs. (20–25). For instance, let $H_0 = 21{,}000$. Then the following are computed:

nutation frequency: $H_0/A_s = 0.442$ rad/sec
maximum average spin axis displacement:

$|2T_x/\dot{\varphi}H_0| = 5.44°$
number of nutation cusps $= |1 - H_0/\dot{\varphi}A_s| = 3.42$/cycle
zero nutation torque angles =
$\dot{\varphi}t_p = |n\pi/[(H_0/A_s\dot{\varphi}) - 1]| = 0°, 105.2°, 210.4°, 315.6°, \ldots n = 0,2,4, \ldots$

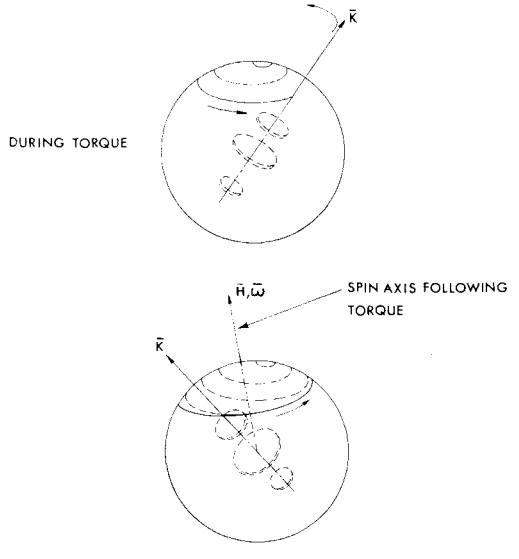

Fig. 5 Spatial response of a nonnutating (spherically configured) system.

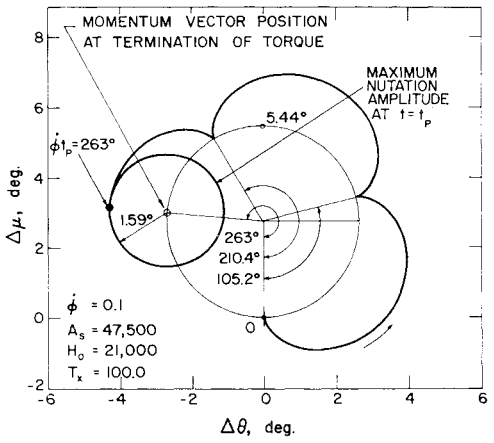

Fig. 6 Theoretically predicted angles in a system with torque termination for which $C_e/A_e > 2$.

maximum nutation =
$\dot{\varphi}t_p = |n\pi/[(H_0/A_s\dot{\varphi}) - 1]| = 52.6°, 157.8°, 263.0°, \ldots$
$n = 1,3,5\ldots$
maximum nutation amplitude is
$2T_x/H_0[\dot{\varphi} - (H_0/A_s)] = 1.59°$ (nutation circle diam $= 3.18°$)

The computer solution for this case is shown in Fig. 6, and it is seen that the foregoing calculations are verified. In Fig. 6, t_p is adjusted to give the maximum nutation amplitude by shutting off the torque at $\dot{\varphi}t_p = 263.0°$. The resulting nutation circle has a radius of 1.59° and is centered on the 5.44° diameter momentum vector circle.

If the system is "stiffened" by spinning up the stages to increase H_0 to +37,000, the number of nutation cusps is calculated to increase to 6.79/cycle, with nutation circles of maximum diameter equal to 0.912° centered on a momentum vector circle 3.1° in diameter. This situation is plotted in Fig. 7a. Similarly, when the system is "softened" by spinning down the stages, the number of nutation cusps per cycle decreases and all amplitudes increase as shown in Fig. 7b for $H_0 = +17{,}000$. Again, all characteristics of the motion

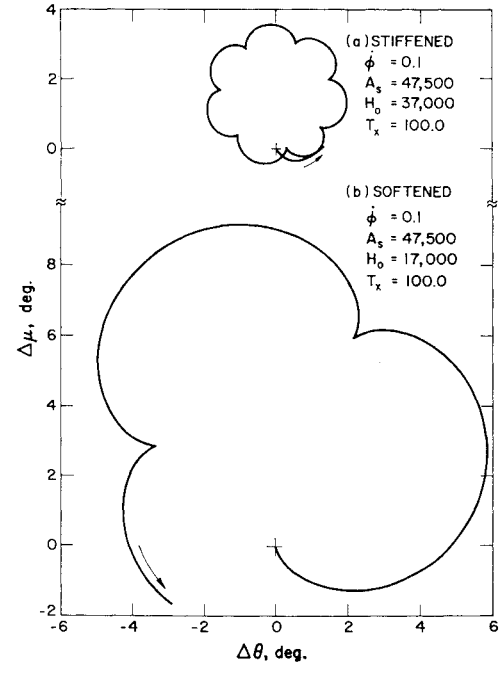

Fig. 7 "Stiffening" and "softening" a system for which $C_e/A_e > 2$.

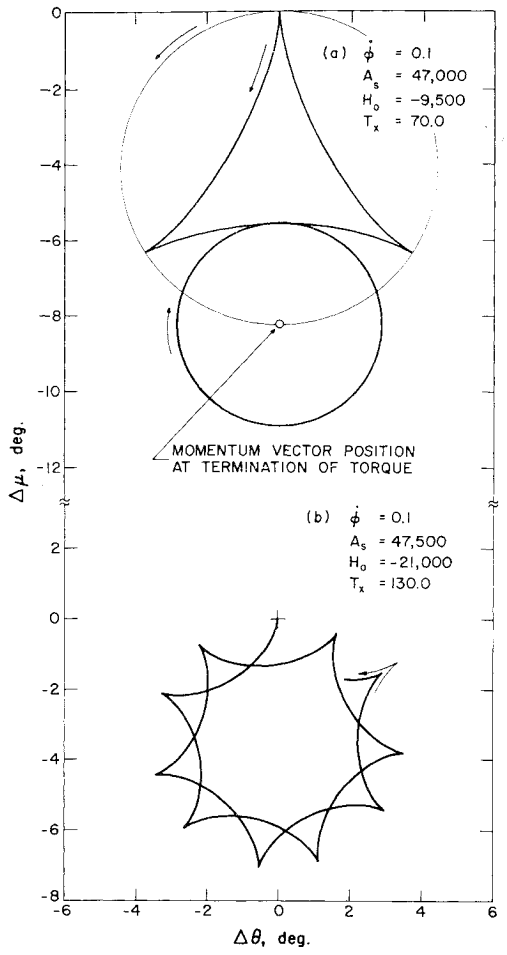

Fig. 8 a) Spin axis motion with nutation for a negative momentum system $C_e/A_e = -2$; b) a "negatively" stiffened system for $C_e/A_e < -2$.

are entirely predictable by Eqs. (20–25).

case 3: $H_0 < 0 (-^{\infty} < C_e/A_e < 0)$

The motion takes on a new form when the spin momentum is made negative relative to the direction of spin of the torquer body. Instead of nutation cusps forming outside the momentum vector circle, they now form inside. Consider the

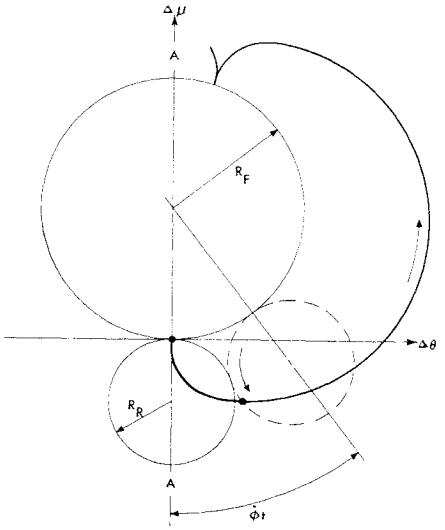

Fig. 9 Graphical method for finding spin axis trace when $1 \leq C_e/A_e < +^{\infty}$.

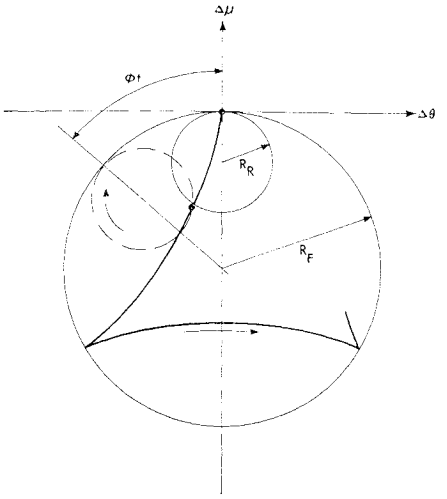

Fig. 10 Graphical method for finding spin axis trace $-^{\infty} < C_e/A_e \leq 1$.

case of $H_0 = -9500 (C_e/A_e = -2)$. Equations (20) reveal that the momentum vector circle has a maximum displacement from the origin of $-8.44°$ and whereas for $C_e/A_e = +2$ (the cardioid of Fig. 4), Eq. (23) gave one nutation cusp, it now predicts three. All this is seen to agree with the solution of the equations of motion as plotted in Fig. 8. In this case, the nutation circles do not pass through the origin. In general, the number of nutation cusps for negative spin momentum will always be two more than the number for positive spin momentum. The same pattern of motion holds if the system is "stiffened" by spinning up the stages in the negative direction as shown in Fig. 8b for $H_0 = -21{,}000$. It is interesting to note in these cases that while nutation frequency H_0/A_s is the same magnitude for positive or negative spin momentum, it changes sign which gives rise to "retrograde" motion for negative momentum and this results in more active nutation and more nutation cusps.

Thus, to a linear approximation, the spin axis motion of any symmetrical coaxial system makes sense and can be logically predicted. It might be expected that such motion could be plotted by a simple graphical technique and such is indeed the case as will be described next.

Graphical Solution of Coaxial System Motion

Since the linearized spin axis motion of the coaxial system in inertial space has been shown to be an epicycloid, a total description of this motion can be derived which simply involves a fixed circle and a point on a rolling circle. Such a graphical method is shown in Fig. 9. The initial conditions are the same as for the derivations, namely stable spin about the axis through the origin at $t < 0$. The fixed circle is the momentum circle defined by Eqs. (20). Its radius is $R_F = T_x/\dot{\varphi}H_0$. The radius of the rolling circle is just half the maximum deviation from the momentum circle found in Eq. (22), or $R_R = |T_x/H_0\xi|$. These circles are initially aligned as in A-A of Fig. 9, and the size of the rolling circle is related to the size of the momentum circle by $R_F/R_R = |\xi/\dot{\varphi}|$. As the system momentum increases, the rolling circle becomes smaller and smaller relative to the momentum circle and the number of nutation cusps correspondingly increases. The number of cusps is equal to the circumference ratio or R_F/R_R which in turn is seen to agree with Eq. (23).

It was shown in the previous section that an equivalent single body unrestricted in inertia ratio can duplicate the motion of any coaxial system during the period while the torque is applied. This analogy will now be used to show how the graphical method applies to any set of coaxial system

parameters.

case I: $+1 \leq C_e/A_e < +^{\infty}$

This case covers the range from an equivalent body of spherical inertia distribution ($C_e = A_e$) to one which nutates infinitely faster than it spins. In this range, the momentum H_0 is in the same direction as $\dot{\varphi}$. For this case, Fig. 9 applies and the rolling circle lies totally outside the momentum circle. The lower limit is equivalent to the condition that $H_0/A_s = \dot{\varphi}$ or $C_e = A_e$. At this limit, the rolling circle is infinitely larger than the momentum circle, and the spin axis continues to diverge as a spiral within the validity of small angle analysis, because a spherical mass distribution which is spinning does not generate gyroscopically stabilizing cross-coupling torques [$C = A$ in Eqs. (1) and (2)]. For the same reason, the body cannot be stabilized against body-fixed torques. As the system momentum increases, the rolling circle diameter decreases until, when the two circles are the same size, the familiar cardioid of Fig. 4 is formed. Further increase in momentum reduces the size of the rolling circle to less than the momentum circle and the number of nutation cusps increases in number as in Figs. 6 and 7.

case II: $-^{\infty} < C_e/A_e \leq +1$

At the upper limit of this range, a transition takes place to a rolling circle that includes the momentum circle as shown in Fig. 10. When $C_e = A_e$ ($H_0/A_s = \dot{\varphi}$), the rolling circle is still infinitely larger in diameter and the same spiral as in case I is formed. Then, however, as $C_e/A_e \rightarrow 0$ (an equivalent body shaped as a long, thin wire, or a coaxial system with no spin momentum), the circles again approach the same diameter which become infinitely large and the spin axis follows the momentum circle as torque angle progresses. This arises from the fact that an ideally thin rod which spins about its long axis cannot be gyroscopically stabilized against either body-fixed or inertially-fixed torques. In this case, A_e is assumed finite, and $C_e = 0$. Now, when the spin momentum goes negative and grows in magnitude, the rolling circle again becomes smaller than the momentum circle and it rolls about inside the momentum circle producing the peaked patterns shown in Fig. 8. For a negative momentum as compared to a positive, with A_s and $\dot{\varphi}$ equals in both cases, the number of nutation cusps is two more for the negative case. This is clear from Eq. (23) and also from the circumference ratio, $R_F/R_R = |\xi/\dot{\varphi}|$.

Conclusions

A linear analysis has been used to describe the spin axis motion in inertial space of a system of coaxial, differentially spinning bodies. The justification for a linear approximation is two-fold: 1) specific parameters which describe the motion are easily isolated and can be applied to any combination of system angular momentum, moment of inertia and torque, and 2) for multispin spacecraft which are reasonably rigid and have high enough angular momentum so that the spin axis motion in inertial space is only a few degrees, a linear analysis is normally adequate.

The coaxial system can duplicate the motion of any single body with a fixed torque of course, but it can also duplicate the motion of a single body which is acted upon by a torque which rotates about the geometric spin axis at a speed (and direction) other than the spin rate. This and other useful "equivalent body" concepts can be used to clarify the elements of motion of seemingly complicated counter-rotating coaxial systems.

These fundamentals reveal that the coaxial system spin axis motion possesses all the properties of an epicycloid which in turn allows this motion to be readily described in clear physical terms by graphical means.

References

[1] Spencer, T. M., "Interactions between a Pointing Control System and the Nutational Motion of a Dual-Spin Spacecraft," *Symposium on Attitude Stabilization and Control of Dual-Spin Spacecraft*, Aerospace Corp., El Segundo, Calif., Aug. 1967.

[2] Landon, V. D., and Stewart, B., "Nutational Stability of an Axisymmetric Body Containing a Rotor," *Journal of Spacecraft and Rockets*, Vol. 1, No. 6, Nov.-Dec. 1964, pp. 682–684.

[3] McElvain, R. J. and Porter, W. W., "Design Considerations for Spin Axis Control of Dual-Spin Spacecraft," *Symposium on Attitude Stabilization and Control of Dual-Spin Spacecraft*, Aerospace Corp., El Segundo, Calif., Aug. 1967.

[4] Simpson, J. O., "The Orbiting Solar Observatory," *Symposium on Attitude Stabilization and Control of Dual-Spin Spacecraft*, Aerospace Corp., El Segundo, Calif., Aug. 1967.